
PICTORIAL ESSAY

Parapharyngeal Space Lesions

DCW Tang, AYH Wan, GKY Lee, JHM Cheng, WK Kan, JLS Khoo

Department of Radiology, Pamela Youde Nethersole Eastern Hospital, Chai Wan, Hong Kong

ABSTRACT

Lesions in the parapharyngeal space are rare and difficult to diagnose and treat. They can arise within the parapharyngeal space or extend secondarily from the surrounding neck area. Differentiation of a parapharyngeal space lesion from a surrounding neck space lesion is essential for differential diagnosis and surgical approach. This pictorial essay discusses imaging features of some common parapharyngeal space lesions.

Key Words: Abscess; Glomus tumor; Neurilemmoma; Pharyngeal diseases; Vascular malformations

中文摘要

咽旁間隙病變

鄧峻樺、尹宇瀚、李家彥、鄭希敏、簡偉權、邱麗珊

咽旁間隙病變是罕見及難以診斷和治療。它們可以源於咽旁間隙或從頸周圍延伸。能夠區別咽旁間隙病變與頸周圍病變對鑑別診斷和手術方法至關重要。本文討論常見咽旁間隙病變的成像特徵。

INTRODUCTION

The parapharyngeal space is a deep-seated space of an inverted pyramid shape extending from the skull base to the greater cornu of the hyoid bone. It is difficult to examine clinically. Differentiation of a parapharyngeal space lesion from a surrounding neck space lesion is essential for differential diagnosis and surgical approaches. Computed tomography (CT) and magnetic resonance imaging (MRI) are the imaging modalities of choice; ultrasonography is less useful for deep-seated lesions.

ANATOMY

The parapharyngeal space is divided into two compartments by a fascia, which extends from the styloid process to the tensor veli palatini (also known as the tensor-vascular-styloid fascia) into the anterior and posterior compartment.¹ The fascia contains the ascending palatine artery and vein. The parapharyngeal space is surrounded by several other spaces of the neck: the pharyngeal mucosal space (medially), retropharyngeal space (posteromedially), and masticator and parotid spaces (laterally). The prestyloid

*Correspondence: Dr DCW Tang, Department of Radiology and Imaging, Queen Elizabeth Hospital, 30 Gascoigne Road, Jordan, Hong Kong.
Email: tcw717@ha.org.hk*

Submitted: 13 Apr 2016; Accepted: 26 Aug 2016.

Disclosure of Conflicts of Interest: As an editor of this journal, GKY Lee was not involved in the peer review process of this article. All other authors have no conflicts of interest to disclose.

compartment includes the branches of the mandibular division of the trigeminal nerve, internal maxillary artery, ascending pharyngeal artery, pharyngeal venous plexus, and minor / ectopic salivary gland, whereas the poststyloid compartment includes the cranial nerves IX to XII, internal carotid artery, internal jugular vein, cervical sympathetic chain, and glomus body.

INFECTIOUS OR INFLAMMATORY LESION

Most infections in the parapharyngeal space either arise from the palatine tonsil or are odontogenic in origin, followed by the submandibular gland and mastoid. On CT, cellulitis appears as fat stranding with fluid density, whereas abscess has a low-attenuation necrotic, pus-filled centre with a thick, irregular enhancing rim. Restricted diffusion is seen on MRI. Other features include intralesional gas pocket and trans-spatial configuration (Figure 1).

NEOPLASTIC LESION

Primary parapharyngeal space tumours (such as neurogenic tumours) are characterised by a fat plane separating the lesion from adjacent neck spaces. Most neoplastic lesions involving the parapharyngeal space are extension from tumours in the surrounding neck spaces, with displacement of the parapharyngeal fat. For tumours arising in the parotid, masticator, carotid, pharyngeal mucosal and retropharyngeal spaces, the parapharyngeal fat are displaced anteromedially, posteromedially, anteriorly, posterolaterally and anterolaterally, respectively. Secondary neoplasms from

surrounding spaces include nasopharyngeal, tongue, and maxilla malignancies, parotid and submandibular gland tumours, lymphomas, glomus tumours, lipomas, and nasopharyngeal angiofibromas.

Neurogenic Tumour

Neurogenic tumours are the most common neoplasm in the poststyloid parapharyngeal space and the second most common neoplasm in the prestyloid parapharyngeal space.² Most of these tumours are schwannomas followed by neurofibromas. Malignant nerve sheath tumours are rare and highly aggressive. Most neurogenic tumours arise from the trigeminal nerve in the prestyloid parapharyngeal space and the vagus nerve in the poststyloid compartment. Solitary neurofibroma is typically a well-defined oval or fusiform low-density lesion, with minimal contrast enhancement. Solitary neurofibroma may be indistinguishable from a schwannoma (Figure 2). Plexiform neurofibromas are poorly circumscribed, locally invasive, trans-spatial lesions with low density.

Salivary Gland Tumour

Salivary gland tumours involving the parapharyngeal space arise either from the deep lobe of the parotid gland (salivary rests within the prestyloid compartment) or the minor salivary glands of the pharyngeal mucosa. Pleomorphic adenoma (Figure 3) is the most common salivary gland neoplasm and appears as an ovoid lesion of soft tissue attenuation. It is typically homogeneous when small, but shows areas of low attenuation when large, indicating cystic degeneration or seromucinous

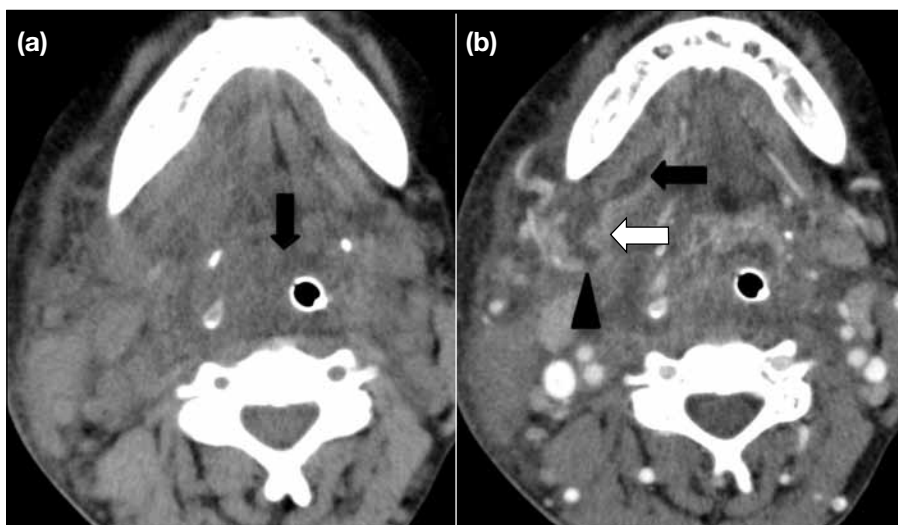


Figure 1. Ludwig's angina complicated with abscess formation: (a) Axial unenhanced computed tomography showing an extensive soft tissue swelling at the supraglottic larynx (arrow) and the adjacent neck spaces, with the endotracheal tube in the narrowed and displaced airway. (b) Axial contrast-enhanced computed tomography showing a rim-enhancing fluid collection in the right submental (black arrow), submandibular (white arrow), and parapharyngeal (arrowhead) spaces; trans-spatial involvement is a characteristic feature of a neck abscess.

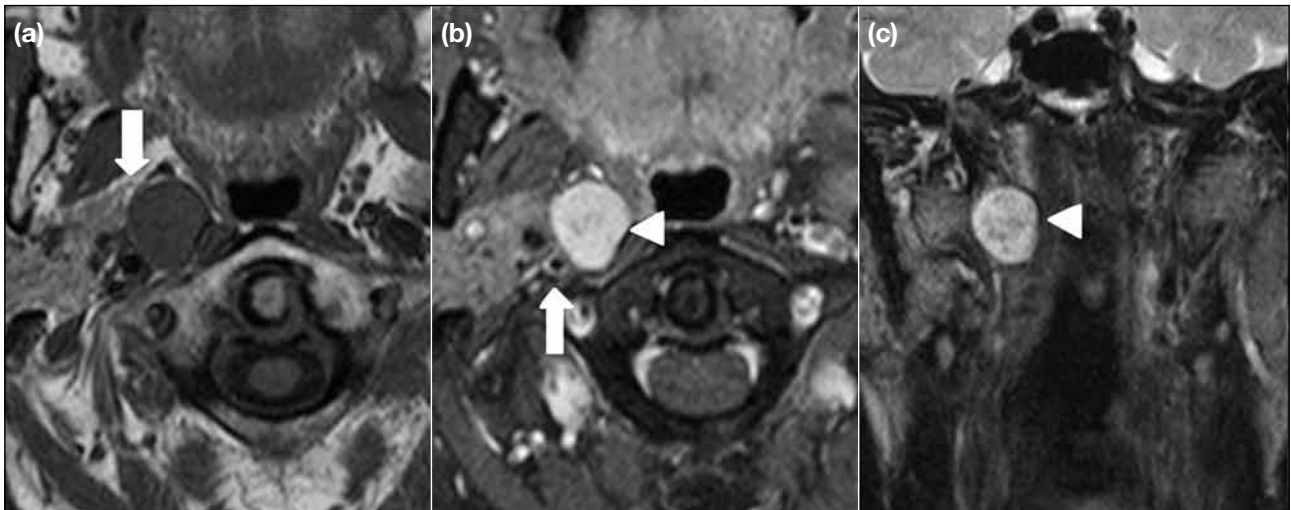


Figure 2. Schwannoma: (a) Axial unenhanced T1-weighted magnetic resonance imaging (MRI) showing a well-circumscribed low-signal-intensity lesion at the right parapharyngeal space, and preservation of the fat plane (arrow) between the mass and the parotid gland. (b) Axial enhanced T1-weighted fat-suppressed MRI showing a homogeneously enhancing mass (arrowhead) located anteromedial to the right internal carotid artery (arrow) with no encasement. (c) Coronal unenhanced T2-weighted MRI showing a well-circumscribed high-signal-intensity mass (arrowhead) without invasion of surrounding structures.

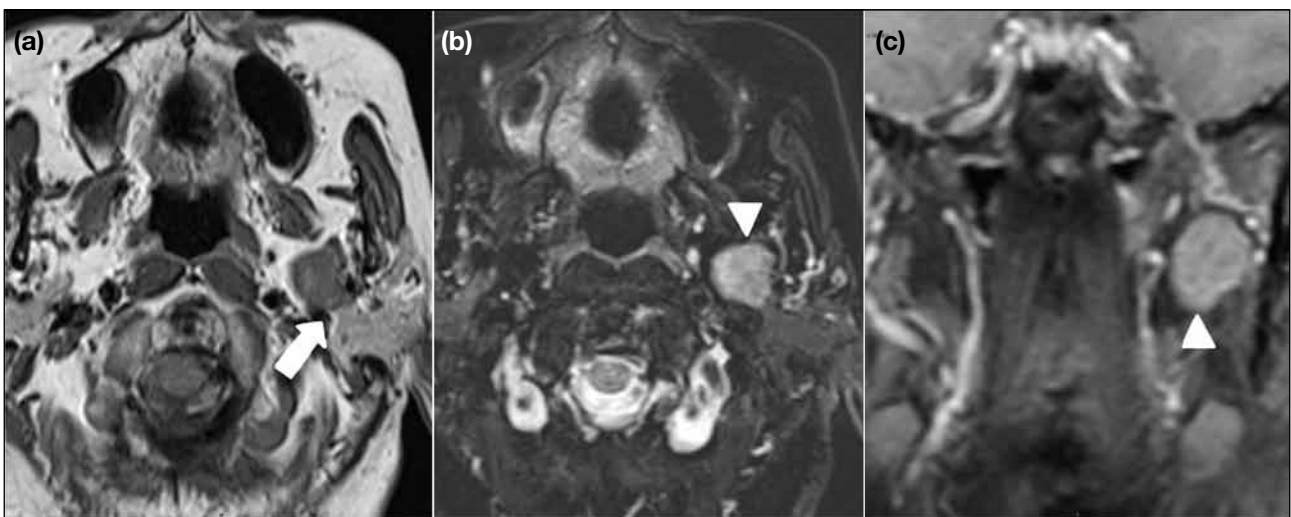


Figure 3. Pleomorphic adenoma of the deep lobe of the parotid gland: (a) Axial unenhanced T1-weighted magnetic resonance imaging (MRI) showing a low-signal-intensity mass at the lateral aspect of the parapharyngeal space. The medial fat plane between the mass and pharyngeal mucosa is displaced but preserved, whereas the lateral fat plane (arrow) between the mass and parotid gland is not seen, indicating that the tumour is parotid in origin. (b) Axial unenhanced T2-weighted MRI showing a high-signal-intensity mass (arrowhead). (c) Coronal enhanced T1-weighted fat-suppressed MRI showing a homogeneous enhancing mass (arrowhead) in the left parapharyngeal space.

collection.³ Pleomorphic adenomas can occur in any age-group but most commonly in those aged 40 to 50 years.⁴ Malignant tumours such as adenoid cystic carcinoma or mucoepidermoid carcinoma are uncommon. Malignant tumours have irregular, ill-defined margins with heterogeneous contrast enhancement and bony destruction.

Glomus Tumour

Glomus tumours are ovoid lesions with well-defined margins showing intense contrast enhancement (Figure 4). Their marked vascularity accounts for the homogeneous avid contrast enhancement. Carotid body tumours typically cause splaying of the internal carotid artery and external carotid artery, whereas

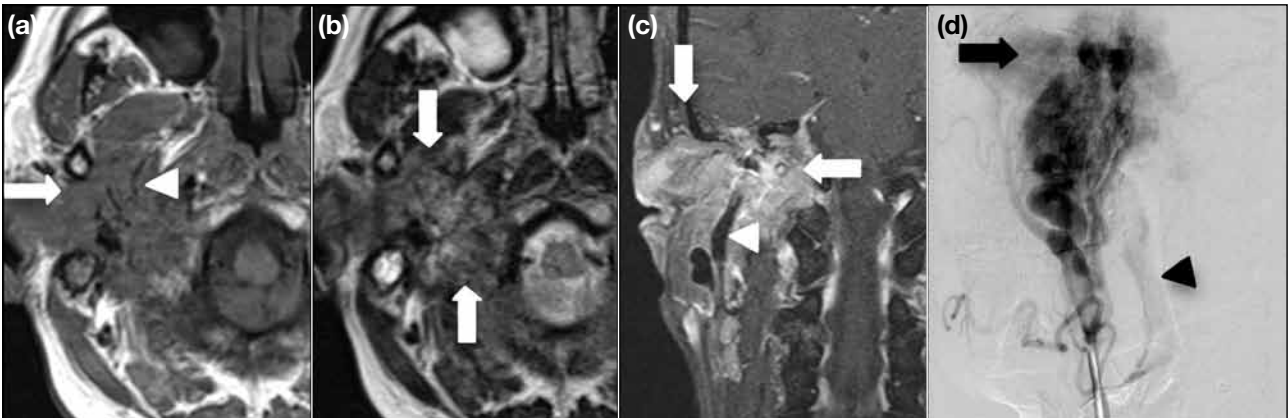


Figure 4. Glomus jugulare: (a) Axial unenhanced T1-weighted magnetic resonance imaging (MRI) showing an isointense mass (arrow) involving the right parapharyngeal and carotid spaces, with multiple intralesional serpiginous flow voids (arrowhead). (b) Axial unenhanced T2-weighted MRI showing a high-signal-intensity mass (outlined by arrows) with internal flow voids. (c) Coronal enhanced T1-weighted fat-suppressed MRI showing a hypervascular mass (outlined by arrows) extending to the right skull base, with the epicentre at the right jugular bulb. Dilated right external carotid arterial branches (arrowhead) are supplying the highly vascularised mass. (d) Right anterior oblique projection of the right external carotid artery by injection digital subtraction angiography showing intense tumour staining (arrow) centred in the right skull base region, with dilated external carotid artery branches. Early venous drainage into the right internal jugular vein (arrowhead) is noted.

glomus vagale tumours typically result in anteromedial displacement of the internal carotid artery without widening of the carotid bifurcation. A ‘salt and pepper’ appearance on MRI is characteristic of glomus tumour owing to tiny foci of haemorrhage and flow voids within the lesion.

Lymphoma

Primary malignant lymphomas of the parapharyngeal space are rare. On CT, lymphomas appear as circumscribed homogeneous lesions isodense to muscle, with mild-to-moderate contrast enhancement, and may display necrosis or calcification after treatment. Lymphomas are typically less infiltrative and cause relatively little bone erosion compared with carcinomas and most sarcomas.⁵ Involvement of the Waldeyer’s ring is an important clue to the diagnosis, as the imaging features of lymphomas are quite non-specific.

Lipoma

Lipomas are the most common benign mesenchymal tumours, with 15% of them occurring in the head and neck region.⁶ There is a bimodal peak of presentation in children and those in the fifth and sixth decades of life. The presence of pain raises the suspicion of malignant transformation.⁷ Lipomas are homogeneous lesions with density similar to subcutaneous fat and without contrast enhancement (Figure 5). Thus, the margin of the lesions

may not be easily distinguishable from the normal parapharyngeal fat.

Nasopharyngeal Angiofibroma

Juvenile nasopharyngeal angiofibromas are rare and benign but locally aggressive, vascular tumours. They account for 0.5% of all head and neck tumours,⁸ and occur almost exclusively in males and usually during adolescence. Juvenile nasopharyngeal angiofibroma appears as a hyperdense mass epicentred within the sphenopalatine foramen, which is widened and typically bowing the posterior wall of the maxillary antrum anteriorly (Holman-Miller sign).⁹ There is avid contrast enhancement due to its high vascularity. On MRI, hypointense flow voids represent enlarged tumour vessels (Figure 6).

Secondary Malignancy from Adjacent Spaces

Neoplastic infiltration of the parapharyngeal space by malignant tumours has been reported. The most common primary malignancy is nasopharyngeal carcinoma, especially in Southeast Asia. Other malignancies include oropharyngeal carcinoma, parotid gland, and maxillary malignancies (Figure 7). Tumours of the skull base such as meningiomas or chordomas can also extend into the parapharyngeal space. By observing the direction of displacement or infiltration of the

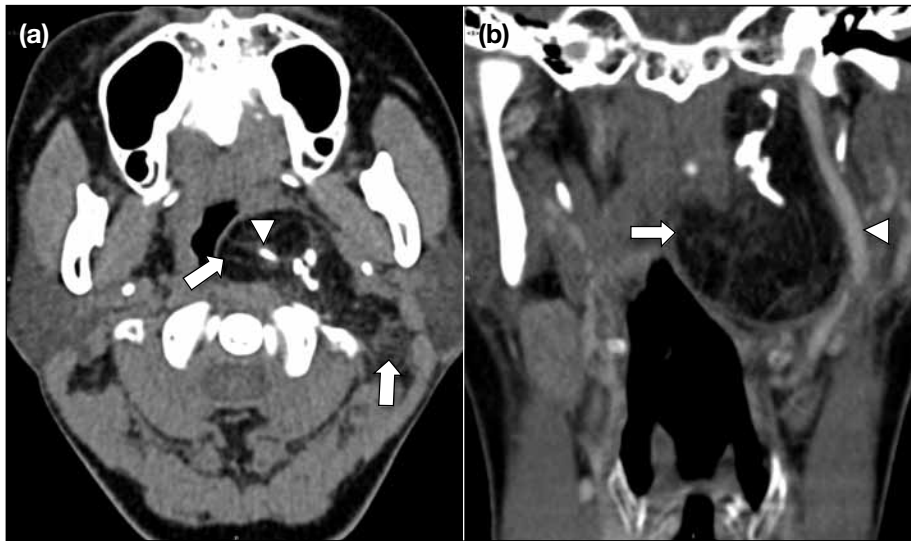


Figure 5. Lipomatous tumour: (a) Axial unenhanced computed tomography showing a well-circumscribed fat-containing lesion (outlined by arrows) with coarse internal calcification (arrowhead) and septation in the left parapharyngeal space. The upper aerodigestive tract is compressed and narrowed. (b) Coronal contrast-enhanced computed tomography showing the fat-containing lesion (arrow) extending up to the skull base, with lateral displacement of the left internal carotid artery (arrowhead).

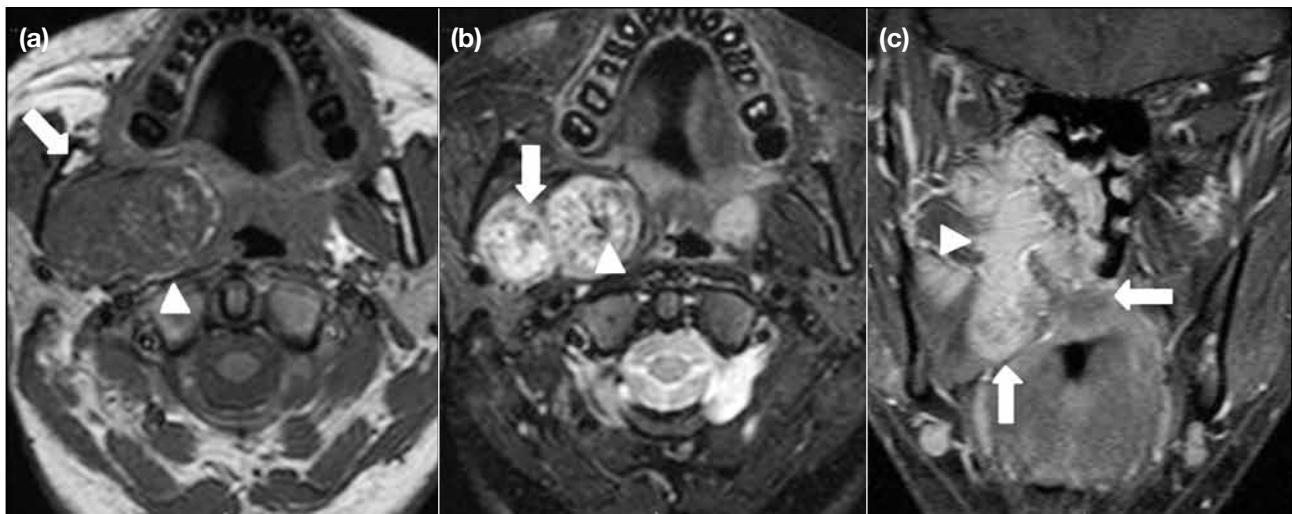


Figure 6. Nasopharyngeal angiofibroma: (a) Axial unenhanced T1-weighted magnetic resonance imaging (MRI) showing a predominantly low-signal-intensity mass (arrow) in the right parapharyngeal space, with several areas of internal high signal intensity. The parapharyngeal fat space is displaced posteriorly (arrowhead) and medially. (b) Axial unenhanced T2-weighted MRI showing a high-signal-intensity mass with septation (arrow) and flow voids (arrowhead) indicating a hypervascular tumour. (c) Coronal enhanced T1-weighted fat-suppressed MRI showing involvement of the nasal cavity, right masticator space, and right parapharyngeal space. Widening of the right pterygopalatine fossa (arrowhead) is characteristic of nasopharyngeal angiofibroma (outlined by arrows).

parapharyngeal space and displacement of the internal carotid artery and internal jugular vein, the lesion can be localised in one of the neck spaces.

VASCULAR ANOMALIES

Vascular anomalies are rare in the parapharyngeal space and include haemangiomas and low-flow vascular

malformations, such as lymphatic malformations and venous malformations (Figure 8).

Lymphangioma

Lymphatic malformations, including lymphangiomas (Figure 9), usually occur in children. Only approximately 10% of lesions are initially present in early

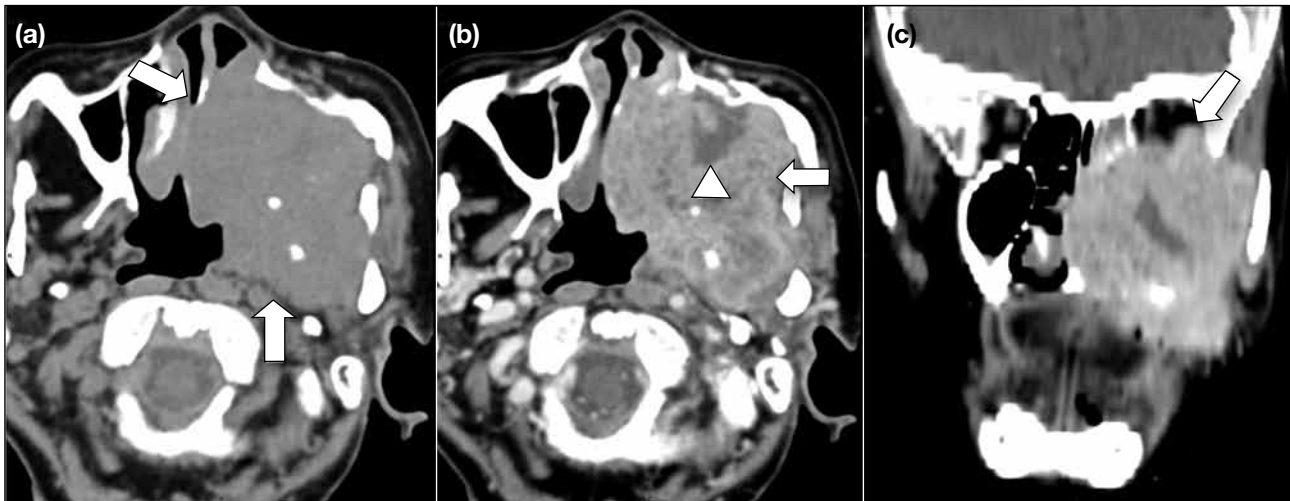


Figure 7. Carcinoma of the maxillary sinus: (a) Axial unenhanced computed tomography showing extensive soft tissue mass (outlined by arrows) at the left maxillary region invading the left nasal cavity, parapharyngeal space, masticator space, pterygoid process, deep lobe of the parotid gland, and left mandibular ramus. (b) Axial contrast-enhanced computed tomography showing the soft tissue mass (arrow) with heterogeneous enhancement and internal hypoenhancing areas (arrowhead) suggestive of necrotic changes. (c) Coronal contrast-enhanced computed tomography showing superior extension to involve the left orbit inferior aspect (arrow) and the ethmoid sinuses.

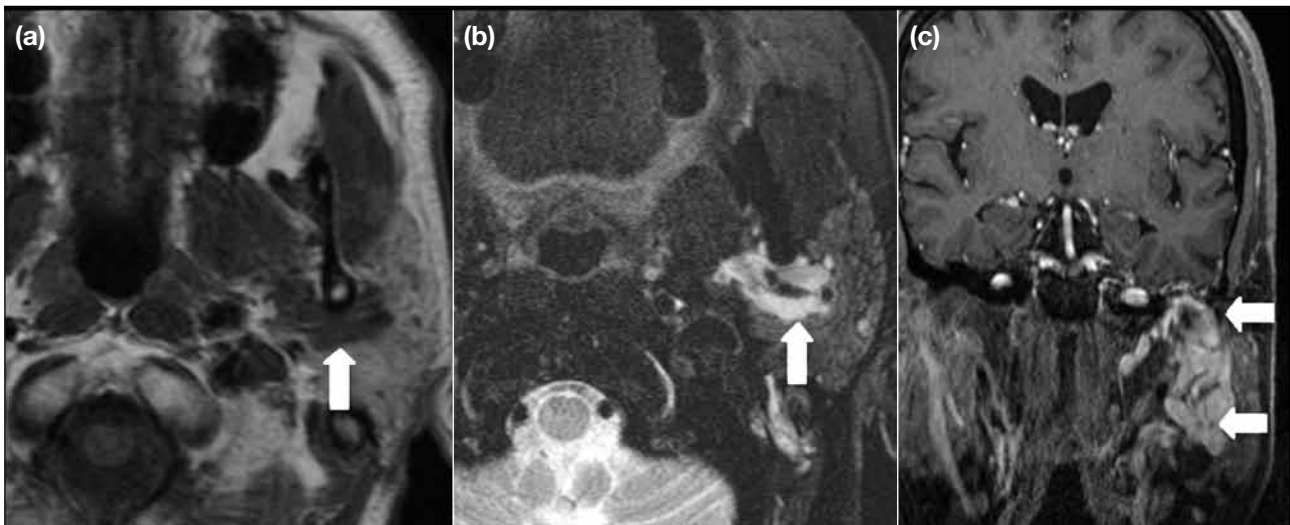


Figure 8. Venous malformation: (a) Axial unenhanced T1-weighted magnetic resonance imaging (MRI) showing a lobulated low-signal-intensity lesion (arrow) posterior to the body of the mandible, extending to the left parapharyngeal space. (b) Axial unenhanced T2-weighted MRI showing a high-signal-intensity lesion (arrow) closely abutting the left parotid gland and the pterygoid muscles. (c) Coronal T1-weighted fat-suppressed MRI showing a serpiginous-enhancing lesion (outlined by arrows) medial to the left parotid gland. The lesion breaches superiorly through the left skull base to the middle cranial fossa and medially to the left parapharyngeal space.

adulthood. They appear as a trans-spatial low-density lesion with no perceptible wall enhancement. Mixed lesions with a prominent vascular component may show variable degrees of enhancement. Lymphatic malformations are benign with no malignant potential.

Recurrence is usually due to incomplete surgical excision.

CONCLUSION

Clinical assessment of the parapharyngeal space is

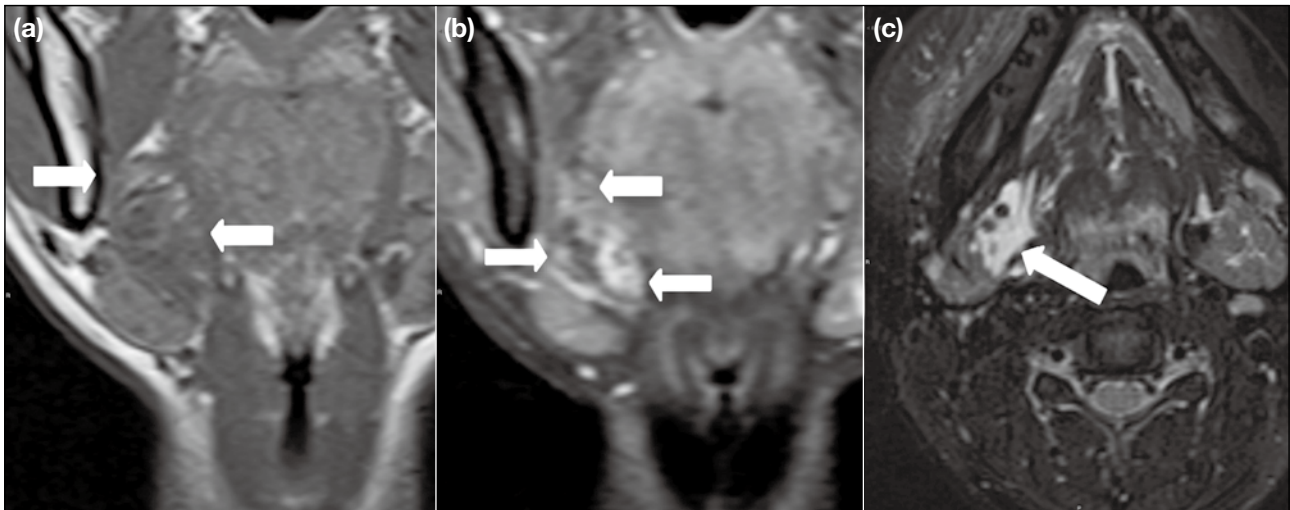


Figure 9. Lymphangioma: (a) Coronal unenhanced T1-weighted magnetic resonance imaging (MRI) showing a low-signal-intensity mass (outlined by arrows) involving the right parapharyngeal and submandibular spaces. (b) Coronal enhanced T1-weighted MRI showing a heterogeneous mass (outlined by arrows) with peripheral enhancement. (c) Axial unenhanced T2-weighted MRI showing a high-signal-intensity mass (arrow).

difficult. Understanding the radiological features of different disease entities in the parapharyngeal space is essential for accurate radiological diagnosis.

REFERENCES

1. Som PM, Curtin HD. Parapharyngeal and masticator space lesions. In: Head and Neck Imaging, Vol 2, 4th Edition. St. Louis: Mosby; 2003. p 1955-87.
2. Tom BM, Rao VM, Guglielmo F. Imaging of the parapharyngeal space: anatomy and pathology. *Crit Rev Diagn Imaging.* 1991;31:315-56.
3. Rajagopal K, Ramesh A, Sreepathi S, Shetty C. CT evaluation of parapharyngeal masses: pictorial essay. *Internet J Radiol.* 2008;10:1-12.
4. Mukherji SK, Chong V. Atlas of Head and Neck Imaging: The Extracranial Head and Neck. New York: Thieme Medical Publishers; 2004. p 413-69.
5. Som PM, Biller HF, Lawson W, Sacher M, Lanzieri CF. Parapharyngeal space masses: an updated protocol based upon 104 cases. *Radiology.* 1984;153:149-56. [cross ref](#)
6. Harnsberger HR, Wiggins RH, Hudgings PA, Michel MA, Swartz J, Davidson HC, et al. *Diagnostic Imaging: Head and Neck.* Salt Lake City: Amirsys; 2006.
7. Mukherji SK, Chong V. Atlas of Head and Neck Imaging: The Extracranial Head and Neck. New York: Thieme Medical Publishers; 2004. p 379-410.
8. Momeni AK, Roberts CC, Chew FS. Imaging of chronic and exotic sinonasal disease: review. *AJR Am J Roentgenol.* 2007;189(6 Suppl):S35-45. [cross ref](#)
9. Garça MF, Yuca SA, Yuca K. Juvenile nasopharyngeal angiofibroma. *Eur J Gen Med.* 2010;7:419-25. [cross ref](#)